Assessing a Generalized CHNO Intermolecular Potential through ab Initio Crystal Structure Prediction

Betsy M. Rice*,† and Dan C. Sorescu‡

The U. S. Army Research Laboratory, Aberdeen Proving Ground, Maryland 21005, and U. S. Department of Energy, National Energy Technology Laboratory, Pittsburgh, Pennsylvania 15236

Received: June 18, 2004; In Final Form: August 31, 2004

We have analyzed a previously proposed [*J. Phys. Chem. B* **1997**, *101*, 798] Buckingham repulsion-dispersion intermolecular potential originally developed for the nitramine explosive RDX using ab initio crystal prediction methods. A total of 174 crystals whose molecules contain functional groups common to CHNO energetic materials were subjected to this methodology. This database includes acyclic and cyclic nitramines, nitrate esters, nitroaromatics, and nitroaliphatic systems. The results of these investigations have shown that for 148 of the 174 systems studied the predicted crystal structures matched the experimental configurations; 75% of these corresponded to the global energy minimum on the potential energy surface. Root-mean-square percent differences between the predicted and the experimental values for the cell edge lengths and densities are about 2 and 4%, respectively. Root-mean-square deviations of rigid body rotational and translational displacements are 2° and 0.07 Å, respectively. Additionally, these same statistics are applicable to the nitramine, nitroaliphatic, nitroaromatic, and nitrate ester classes, suggesting that this interaction potential is transferable across these classes of compounds. The success rate in predicting crystals with structural parameters and space group symmetries in agreement with experiment indicates that this method and interaction potential are suitable for use in crystal predictions of similar CHNO systems when the molecular configuration is known.

1. Introduction

This is the ninth in a series of papers describing our development and assessment of interaction potentials to be used in the study of dynamic processes in energetic materials. The model under assessment was originally developed to study nonreactive processes in the nitramine explosive RDX (1,3,5-hexahydro-1,3,5,-*s*-triazine)[1] and will be denoted hereafter as the SRT potential or model. Its form is a simple Buckingham, $A\exp(-Br) - C/r^6$, (exp-6) function plus Coulombic interactions. The Coulombic interactions were determined through fitting atom-centered partial charges to a quantum-mechanically determined electrostatic potential for a single RDX molecule whose structure corresponded to that in the crystal at ambient conditions. The nonbonding parameters were fitted to reproduce crystallographic parameters and lattice energy for RDX at ambient conditions.

In the original fitting of the SRT potential, the C−C and H−H homoatom potentials were taken from the hydrocarbon force field developed by Williams.[2] For N−N and O−O homoatom potential parameters, the *B* factors of the Buckingham potentials given by Williams[2] were also used, whereas the corresponding *A* and *C* Buckingham potential parameters were fitted using information about the observed crystalline structure of RDX at room conditions. The heteroatom potential parameters were determined from homoatom parameters using traditional combination rules, namely the geometric mean for *A* and *C* potential terms and the arithmetic mean for *B* terms. Additionally, the energy of the RDX crystal, determined using the experimental enthalpy of sublimation, was also used in the fitting procedure to determine the necessary set of potential parameters.

An initial assessment of the SRT potential was performed through molecular packing (MP) calculations and isothermal isobaric molecular dynamics (NPT-MD) simulations of RDX at room temperature and ambient pressure.[1] The results of these calculations have shown that simulated crystal structures at 300 K were in outstanding agreement with experiment, within 2% of lattice dimensions and almost no rotational and translational disorder of the molecules in the unit cell. Moreover, it was confirmed that the crystallographic space group symmetry was maintained both in molecular packing calculations as well as during the MD trajectory simulations where thermal effects were present.

Following this initial study, in a series of successive papers, we assessed the degree of transferability of this potential to predict properties of other molecular crystals. Based on molecular packing calculations we have shown that for a wide variety of CHNO crystals with functional groups common to energetic materials, the SRT force field is transferable.[3−7] Particularly, we considered a large database which included 30 nitramine crystals[3−5] and 51 other CHNO molecular crystals comprising a wide variety of compounds such as nitroalkanes, nitroaromatics, nitrocubanes, polynitroadamantanes, polynitropolycycloundecanes, polynitropolycyclododecanes, hydroxynitro derivatives, nitrobenzonitriles, nitrobenzotriazoles, and nitrate esters.[6] The crystals in both these sets encompassed acyclic, monocyclic, and polycyclic molecules. Beside RDX, other important energetic materials considered in these studies were HMX (octahydro-1,3,5,7-tetranitro-1,3,5,7-tetraazacyclooctane), different polymorphs of CL-20 (2,4,6,8,10,12-hexanitrohexaazaisowurtzitane), various nitrocubanes (1,4-dinitrocubane,

* To whom correspondence should be addressed.
† The U. S. Army Research Laboratory.
‡ National Energy Technology Laboratory.

10.1021/jp047334l
Published on Web 10/21/2004

1,3,5-trinitrocubane, 1,3,5,7-tetranitrocubane, and 1,2,3,5,7-petanitrocubane), PETN (pentaerythritol tetranitrate), and TNT (2,4,6-trinitrotoluene). MP calculations using the SRT interaction potential reproduced the crystal lattice dimensions to within 2% for most of the 30 nitramine crystals and within 3% of experimental data for most of the 51 nonnitramine systems. NPT-MD simulations at ambient and moderately high pressures (5−10 GPa) were also performed for a few important energetic molecular solids, including RDX, HMX, CL-20, and PETN in order to assess the performances of the SRT force field in prediction of the hydrostatic compression effects within the rigid molecule approximation.[7] For all of these systems, the predicted crystallographic parameters at pressures below 5 GPa were found to be within a few percent of the experimental values. Furthermore, the crystalline space group symmetries were maintained in the simulations. However, in the regime of higher pressures, above 6 GPa, simulations for floppy systems such as PETN produced results that were in a larger disagreement from experimental values. This indicates that for these floppy systems the rigid-body approximation is inadequate for use in the high-pressure regimes.

Although the SRT model appears to be a promising candidate of a generalized interaction potential for use in molecular simulation of CHNO molecular crystals, increasingly rigorous assessments should be performed to establish the limits of the model's capabilities and provide information for refinement. Particularly, it is important to establish whether such a potential is able to reproduce the crystal structure and the corresponding lattice energy known from experimental data and also to predict the crystallographic symmetry without its prior knowledge. The study presented here provides such an assessment. In this work, we have subjected a series of CHNO crystals that are representative of different classes of explosives to ab initio crystal structure prediction using the SRT interaction potential. Our major goal in this investigation is to evaluate the performance of the SRT potential for the case of CHNO systems in generating hypothetical crystal structures that are consistent with those observed experimentally.

The calculations we present in this work are similar to the previously described molecular packing (MP) calculations for a variety of CHNO molecular crystals[1,3−6] except for the following details. In the earlier calculations, the initial structures used for the energy minimization of a MP calculation corresponded to the experimental structure. Therefore, only a small region of configurational interaction space of the system was sampled during these MP calculations. Although the resulting MP predictions were in good overall agreement with experimental values, they did not indicate whether other local minima with the same or with different crystal symmetries exist on the potential energy surface and if the experimentally observed geometry corresponds to the absolute minimum on the potential energy landscape. The calculations presented here will allow us to investigate a wider region of the configuration space for our model potential. This is done by performing a large number of MP calculations for a molecule placed in various orientations within a unit cell and for a wide variety of crystalline symmetries. Moreover, to make this analysis even more comprehensive, we have significantly extended the database of CHNO compounds[1,3−7] investigated but still limit ourselves to the case of chemical systems of interest for energetic materials applications. In particular, in this work, we have considered compounds containing nitramines, nitrate esters, nitroaliphatics, nitroaromatics, and furoxans.

Organization of this paper is at follows: Section 2 gives the experimental crystallographic information used in the study, and section 3 describes the potential energy function that is used to represent the intermolecular interactions of the corresponding crystals. Section 4 provides a description of the ab initio crystal structure prediction methods and the capabilities of the molecular packing program used in this study, MOLPAK/WMIN.[8−9] In section 5, we will describe and discuss the results of our ab initio crystal prediction calculations for the entire set of 174 compounds from different chemical classes of CHNO crystals. Summary and concluding remarks are provided in section 6.

2. Experimental Data Used in the Study

The structural data of the molecular systems considered in this study were obtained from the Cambridge Structural Database (CSD).[10] No modifications to the experimental structures were made. The main categories of compounds used were species having nitro groups attached to carbon (denoted as nitroaliphatic or nitroaromatic), nitrogen (nitramine), or oxygen (nitrate esters). Additionally, a few furoxan systems were considered. Within this paper, systems will be referred to by their CSD entry identifier (*refcode)*.[10] Structures were eliminated from consideration for this study if:

1. The space group could not be treated by MOLPAK calculations. We did not exclude crystals with space groups that were alternate settings of those that could be treated by the version of MOLPAK used in this study.
2. The systems contained atoms other than C, H, N, and O.
3. The systems contained solvent molecules.
4. There is more than one molecule in the asymmetric unit.
5. Those systems in which the asymmetric unit contains only part of the molecule and no C2 rotation axis or center of inversion exist among the symmetry elements of the crystal. However, when such symmetry elements are present, the corresponding crystals can be considered for MOLPAK simulations.
6. Fractionals for some or all of the non-H atoms were not available. However, a few systems for which some or all of the hydrogen atoms were not available (BEYDOY, DEFLEF, AND GEJXAU) were still included in this study. To calculate the packing for these systems the hydrogen atoms were added at ideal positions using the Gaussview visualization package.[11]
7. Systems that have disordered atomic positions or have crystallographic R-factors greater than 11%.

This search, which was not exhaustive, resulted in the identification of 174 molecular crystals that represent our working database to be subjected to ab initio crystal prediction. Information about these, including full chemical name, CSD *refcode*, chemical formula, space group, temperature at which measurements were taken, and reported R-factors are given in Table 1S.

3. Intermolecular Potential

We have assumed that the potential energy used in this study for a system of N molecules can be described as the sum of intermolecular interaction terms

$$V^{\text{Total}} = \frac{1}{2}\sum_{i=1}^{N}\sum_{j=1}^{N} V_{ij}^{\text{intermolecular}} \qquad (1)$$

The intermolecular potential is the same as described in the earlier studies[1,3−7] and consists of the superposition of a pairwise

sum of Buckingham (6-exp) (repulsion and dispersion) and Coulombic (C) potentials of the form

$$V_{\alpha\beta}(r) = A_{\alpha\beta} \exp(-B_{\alpha\beta} r) - C_{\alpha\beta}/r^6 \quad (2)$$

and

$$V^C_{\alpha\beta}(r) = \frac{q_\alpha q_\beta}{4\pi\epsilon_0 r} \quad (3)$$

where r is the interatomic distance between atoms α and β, q_α and q_β are the electrostatic charges on the atoms, and ϵ_0 is the dielectric permittivity constant of free space. The parameters $A_{\alpha\beta}$, $B_{\alpha\beta}$, and $C_{\alpha\beta}$ for different types of atomic pairs have been previously published and have been used in the present study without change.[1]

The set of partial charges used in these calculations was determined through fitting these to the quantum-mechanically derived electrostatic interaction potential for an isolated molecule whose atoms are arranged in the experimental crystallographic arrangement. These calculations have been done using the CHELPG procedure as implemented in the Gaussian 03 package.[11] Our earlier studies demonstrated that for the majority of the crystals studied, the best agreement between simulations and experiment occurs when the set of partial charges is determined using methods that employ electron correlation effects.[5−6] Due to the number and sizes of the systems under study, we used partial charges determined using the nonlocal density functional theory and the B3LYP density functional[12,13] and the 6-31G** basis set.[14] Although the accuracy of the earlier MP calculations using the B3LYP/6-31G** charges were not as good as those obtained using charges calculated with the more computationally demanding second-order Möller−Plesset (MP2) theory,[15−20] MP calculations using B3LYP/6-31G** charges give a reasonable representation of the crystallographic parameters and the corresponding lattice energies. These findings, coupled with the large number and sizes of the molecular systems requiring ab initio determination of partial charges and to our desire to make this procedure useful to users who might have limited computational resources, made the option of using B3LYP/6-31G** preferable.

4. Computational Methods

4.1. Crystal Structure Prediction. An ideal ab initio crystal structure prediction method should lead to identification of the most thermodynamically and kinetically favorable crystal structure using only the theoretical information about a single molecule. However, practical limitations on current methodologies and implementations preclude the achievement of this goal.[21−26] These limitations include the elimination of kinetic considerations when ranking possible candidate crystals due to an inability to theoretically treat kinetic factors associated with crystal growth, such as solvent effects and crystallization conditions. Additionally, the majority of computational methods assume that the crystal structure with the lowest lattice energy corresponds to the thermodynamically favored structure rather than the structure with the lowest free energy. This assumption effectively ignores entropic and vibrational enthalpic contributions to the free energy. Additionally, any ranking based on lattice energies is completely dependent on the quality of the description of the intermolecular interactions, which, in almost all cases, are empirical functions parametrized using limited experimental information. Some methods (including those used in this study) restrict the molecular models used in the structure generation and packing calculations to be rigid. This restriction does not allow for the deformation of the molecular model by crystalline forces and may affect the final result. Despite these constraints, the utility of the current methods designed for crystal prediction is not lessened, since the calculations generate a set of low-energy crystal structures that usually include the experimental structure (assuming good models of the intermolecular interactions and the molecular structure are used). Such hypothetical crystal structures can aid in the determination of the real crystal structure for cases in which the measurements do not lead to definitive results.[8,31−34] This is accomplished through the comparison of simulated powder diffraction spectra for candidate systems with the experimental data. Further, ab initio crystal prediction calculations can be used to assess the quality of an intermolecular interaction potential such as that presented herein.

In this study, we wish to determine whether crystal structure predictions using the SRT interaction potential for the CHNO system will generate crystals whose structural parameters and space group symmetries are in agreement with experimental data without prior knowledge of the crystalline information. This data will provide the user with a confidence level in the model. Finally, once the confidence level of the model is established, the method can be used to rapidly screen a wide variety of notional candidate materials for applications in which crystal morphology or density are critical indicators of activity and performances of these materials.[23] This is particularly important for energetic materials where the density of a material is a key indicator of its detonation properties and of its performance in a gun under idealized firing conditions. Although absolute identification of the experimental structure cannot be guaranteed from these calculations, the generation of a series of low-energy hypothetical crystal structures will provide a materials designer with a range of density values that should allow for screening of the materials. The elimination of less promising materials identified through such calculations will reduce waste streams associated with unnecessary synthesis and measurements and will allow time and pecuniary resources to be expended on the more promising candidates.

4.2. MOLPAK/WMIN Crystal Structure Prediction Method. In our study, we have used the ab initio crystal structure prediction software MOLPAK/WMIN,[8−9,31] developed with an emphasis on density predictions of energetic materials. A key assumption in the MOLPAK/WMIN procedure is that of closest packing of the molecules in the crystal;[8,27] the procedure attempts to identify structures with the highest densities. The MOLPAK portion of the calculation generates numerous candidate crystal structures of minimum volume for molecular coordination geometries observed in the most common space groups. MOLPAK considers 29 coordination geometries for the triclinic (P1, $P\bar{1}$), monoclinic ($P2_1$, $P2_1/c$, Cc, C2, $C2/c$), and orthorhombic (Z = 4, $P2_12_12$, $P2_12_12_1$, $Pca2_1$, $Pna2_1$ and Z = 8, *Pbcn*, *Pbca*) space groups. A subset consisting of the most dense candidate crystals are subjected to further refinement through full energy minimization using the program WMIN.[9] The steps in the procedure are as follows:

1. The Cartesian coordinates of the three-dimensional molecular model that is to be used in building the candidate crystals (hereafter referred to as the "test molecule") are specified. The centroid of the test molecule is located at the origin of the hypothetical crystal. The orientation of the molecule is given by a set of Euler angles. In this study, the arrangement of the atoms in the molecule corresponds to that of the crystal molecular structure, as reported in the CSD.[10]

2. An initial packing arrangement is obtained by surrounding the test molecule with a coordination sphere containing other molecules. The contents and three-dimensional structure of the sphere are dependent on the crystalline space group symmetry. The definitions of the various coordination spheres used in a MOLPAK calculation were obtained from detailed analyses for a large number of organic crystal structures.[8] The analyses showed that the most probable number of molecules in the coordination sphere is 14, and that specific "patterns and subpatterns" were apparent in the three-dimensional structure of the coordination spheres.[8]

3. Adjacent molecules in the coordination sphere are then systematically moved in small steps toward the centrally located test molecule. At each step, the potential energy of the "crystal" is calculated. This continues until a repulsion criterion is met. Once this criterion is met, the packing procedure stops, and the volume, crystallographic parameters, and Eulerian angles that describe the orientation of the test molecule are stored.

4. The test molecule is then reoriented about only one of the Eulerian axes by 10°, and the packing procedure (steps 1−3) is repeated until the entire Eulerian space is sampled. Rotations in 10° steps about the three Eulerian axes will result in the generation of 6,859 (19^3) orientations and hypothetical crystal structures for each of the possible space group/coordination sphere combinations.

5. After the ~7000 structures were generated for each coordination sphere geometry, they are ranked according to density. The 25 most dense structures are subjected to full energy minimization, where minimization is performed with respect to the crystallographic parameters. The energy minimization is space-group symmetry restricted (i.e., the space group symmetry is conserved throughout the minimization) and performed using the code WMIN.[9]

At the completion of the energy minimizations of the 25 most dense hypothetical crystals generated for each of the 29 space group/coordination-sphere geometries, the user has the information needed to identify the "correct" crystal structure according to his specific criteria (e.g., lowest lattice energy or highest density[27]). During energy minimizations, some of the hypothetical crystals can converge to the same local minimum on the PES. However, identical crystals have not been eliminated in the analyses reported hereafter.

The MOLPAK/WMIN procedure proceeds under the assumption that all important regions of configuration space are adequately sampled and that the interatomic interactions are sufficiently accurate to describe packing and lattice energies. Unfortunately, we found that in some cases the MOLPAK/WMIN procedure did not result in the identification of the experimental structure. For those cases, a second MOLPAK/WMIN series of calculations were performed in which the test molecule was reoriented about each of the Eulerian axes in increments of 5°, resulting in the generation of 50 653 (37^3) orientations and a corresponding larger number of hypothetical crystal structures. For a number of structures, the increased resolution of the grid led to successful identification of the corresponding experimental structures.

4.3. Method of Comparison of Structures. The comparison of crystallographic structures predicted using the MOLPAK/WMIN codes with experiment was accomplished in a series of steps. The first step is the comparison of the reduced cell parameters obtained from MOLPAK calculations with the corresponding experimental values. The MOLPAK crystal with reduced cell parameters that most closely agree with experimental values is identified as a potential match. Reduced cell parameters are compared because they give a unique representation of a crystal lattice;[32] conventional cell representations are not necessarily unique in their representations of the lattice. Although this preliminary identification step uses reduced cell parameters, the results herein, reported in the supplemental Tables 3S and 4S, are given in the conventional setting, for convenience to the reader.

A more rigorous comparison of crystals has been performed to check that not only the lattice parameters are in agreement with experimental values but also the arrangement and orientation of molecular systems inside the unit cell resemble the experimental situation. The first step of this portion of the assessment is the generation of the experimental unit cell and a MOLPAK supercell consisting of 125 unit cells ($5 \times 5 \times 5$ unit cells). Next, the experimental unit cell and MOLPAK supercell are translated such that the mass centers of the central molecule of the MOLPAK supercell and one of the molecules in the experimental unit cell are located at the origin. Using the procedure described by Kearsley,[33] the MOLPAK supercell is then rotated about the origin such that the central molecule of the MOLPAK supercell is superimposed onto the experimental molecule. Since the molecular structures used in the MOLPAK calculations are exactly the same as those in the experimental unit cells, the Kearsley procedure will result in a perfect superposition of the MOLPAK and experimental molecules. At this point, the molecules in the MOLPAK supercell that correspond to each of the remaining equivalent molecules in the experimental unit cell are identified by minimizing the root-mean-square (rms) deviation of distances between the two sets of molecules. Once the MOLPAK unit cell that most closely resembles the experimental unit cell is obtained, the MOLPAK and experimental unit cells are shifted such that the mass centers of both cells are located at the origin. The Kearsley procedure[33] is then applied using all molecules within both unit cells, to obtain optimum superposition of the MOLPAK unit cell onto the experimental cell. Locations of mass centers and orientations of all molecules in both experimental and predicted unit cells are calculated and compared; the corresponding results are given in Table 3S. Orientations of the molecules are described in terms of the Euler angles used to rotate the Cartesian coordinate axes onto those of the principal axes of each molecule. Factors $\Delta\theta$ and Δx in Table 3S are the total rms rigid-body rotational displacement (in degrees) and translational displacement (in Å) after minimization. Finally, a visual comparison of the superimposed unit cells is performed to confirm that the MOLPAK unit cell resembles the experimental cell.

5. Results

The ab initio MP results obtained for the entire set of 174 molecular crystals are compiled in Tables 1S−4S. In Table 1S, we present the crystallographic and nomenclature information for each molecular crystal considered in this study. In addition, we indicate in this table whether the MOLPAK calculations produced a structure that is considered to be a match with experiment and if this matching structure has the lowest energy among the entire set of hypothetical structures. In Table 2S for each system investigated, we provide several types of data. First we indicate the lattice energies of the global minimum (GM) found and of the structure which represents the match of the corresponding experimental configuration. This last type of structure will be denoted in the following as "the match". In the majority of cases, the global minimum coincides with the match to experiment and as a result the two energies are identical. We also indicate in Table 2S the energy gap between the global minimum and the next local minimum with energy

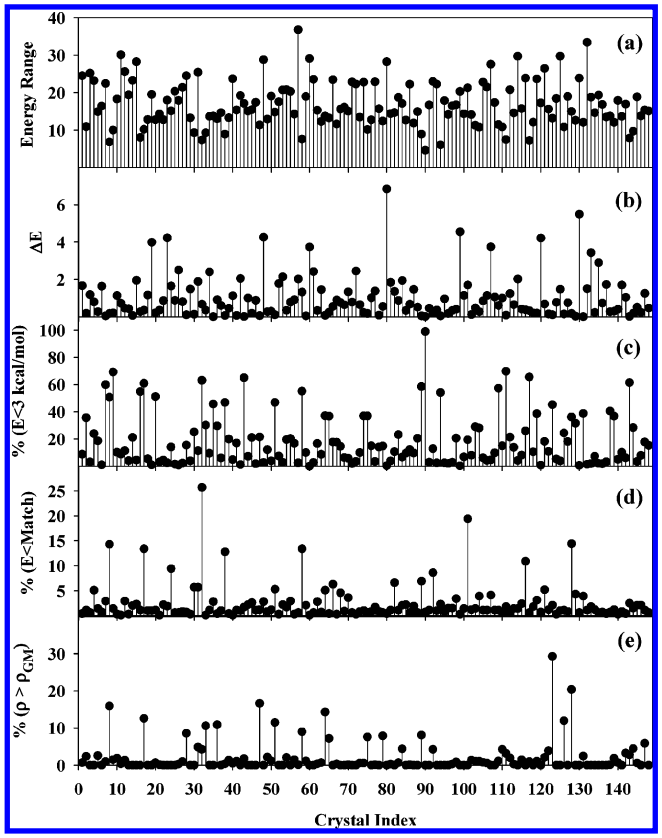

Figure 1. (a) Energy range of the hypothetical crystals generated for each system; (b) The energy gap ΔE between the global minimum (GM) and the local minimum with energy closest to the GM; (c) Percentages of systems that are within 3 kcal/mol of the GM; (d) Percentages of systems that have lattice energies lower than the structure that matches the experiment; (e) Percentages of systems with densities higher than that of the GM. The crystal indices for each frame correspond to those given in Table 2S. The energy units are kcal/mol.

closest to the GM determined from the entire set of hypothetical crystal structures of a particular system. Column 6 of Table 2S indicates for each particular case the energetic range sampled by the corresponding hypothetical crystal structures. We analyze in columns 7 and 8 the percentage of crystals with energies smaller than that of the match structure and with energies within 3 kcal/mol from the GM. Finally, the last column in Table 2S provides the percentage of crystals with energies within 3 kcal/mol of GM and with densities greater than the one determined for the structure at the global minimum. Representative data contained in Table 2S is also provided in Figure 1 for easy interpretation and analysis.

The ranges of lattice energies relative to the GM for the various hypothetical crystals are represented in Figure 1a. It can be seen that there is a relatively large spread of the energetic ranges with values between 4.6 kcal/mol to nearly 40 kcal/mol. It has been recommended that structures with lattice energies that are more than 3 kcal/mol higher than that of the GM should not be considered as probable structures;[28] therefore, for those systems in which the energy ranges are quite large, the higher-energy crystals can be discarded from consideration. Furthermore, it has been proposed that for those cases in which the lattice energy of the match to experiment is the GM, a significant energy gap between the GM and all other crystals indicates "a readily predicted robust crystal structure".[26] The corresponding energy gaps obtained in our simulations are presented in Figure 1b. As indicated by this figure, the gap energies have values below 2 kcal/mol for the great majority of crystals investigated indicating the presence of closely spaced local minima in the region of the GM. Also, as evident from Table 2S and Figure 1b, there are several cases in which the hypothetical crystals have lattice energies that are almost equal to the GM, even though upon inspection the crystal parameters were often quite dissimilar (e.g., different space groups, different orientations of the molecules within the unit cell).

A similar finding emerges from the analysis of the data illustrated in Figure 1c where the percent of hypothetical crystals with lattice energies within 3 kcal/mol of the global minimum is represented. Indeed, it can be observed that for many systems a large number of the hypothetical crystals are distributed in a relative narrow energy window above the GM.

As shown in Figure 1d where the percentages of crystals that are lower in energy than the matches are given, the hypothetical crystal selected as the match to the experimental structure is, in most cases, among the lowest-energy crystals generated in the MOLPAK/WMIN procedure. The most notable exceptions are DNEDAM (*N*,*N*′-dinitroethylenediamine, entry 32 in Table 2S) and PERYTN01 (pentaerythritol tetranitrate, entry 101 in Table 2S), which had lattice energies higher than the GM by 1.45 and 2.86 kcal/mol, respectively.

A previous survey study of crystalline polymorphs showed that in most cases polymorphs with higher densities have correspondingly lower lattice energies.[34] We have investigated this point and the corresponding results are presented in Figure 1e. In this figure, we represent the percentage of hypothetical crystals with densities greater than that of the structure corresponding to the GM. As indicated in Figure 1e, we observe that in majority of analyzed cases systems having the highest density correspond to the GM, whereas a relatively small number of crystals have densities in excess of that of GM. The most notable exceptions are for TIJKEC (1-amino-2-nitraminoethane, entry 123 in Table 2S) and VIMHEE10 [bis-(nitratopropyl)oxamide, entry 128 in Table 2S]. The hypothetical crystal for TIJKEC that best matched the experiment was not the low-energy structure and had a lattice energy higher than that of the GM by 0.28 kcal/mol. Despite this relatively small energy difference for the TIJKEC system, there were 29% of other hypothetical crystal structures that had energies within the 3 kcal/mol range from the GM and densities higher than that of the GM. Similarly, in the case of the VIMHEE10 crystal, the global minimum identified by MOLPAK/WMIN analysis was found to match the experimental structure but about 20% of the other alternative crystal structures had densities higher than that of the GM.

One of the systems having a GM with structural parameters in good agreement with experiment and with a significant energy gap between the GM and all of the other hypothetical crystals is CTMTNA (RDX, cyclotrimethylene-trinitramine, entry 22, Table 2S). In this case, there is also a moderate range of spread of energies (12.75 kcal/mol) for various hypothetical structures. The predicted densities and the corresponding lattice energies for all local energy minima identified are shown in Figure 2. In this case, the difference in energy between the GM and all of the other crystals is 0.87 kcal/mol (see Table 1). The next local minimum above the GM has the same space group symmetry as the experimental structure and has crystallographic parameters that deviate from the experiment by only a few percent (Table 1). However, the rms rigid body rotational and translational displacements for this structure are large, and the pictorial representations of the hypothetical crystal superimposed onto the experimental unit cell confirmed that this higher-energy crystal could not be considered as a good match for this system. For the RDX system, only 4.6% of the crystals have energies

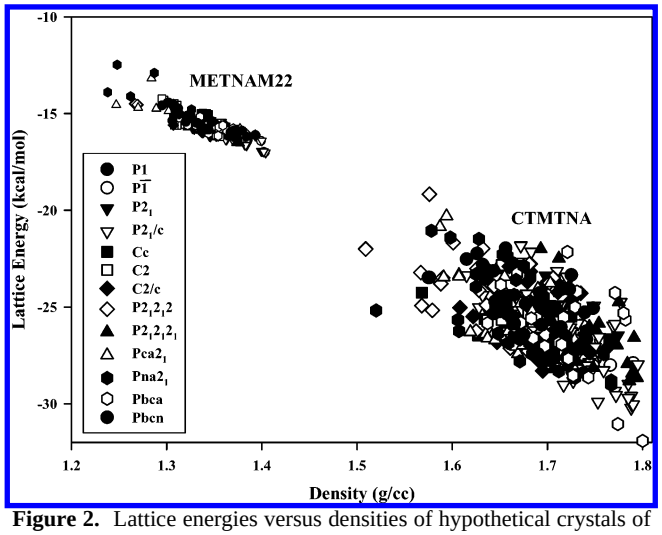

Figure 2. Lattice energies versus densities of hypothetical crystals of METNAM22 and CTMNA generated by ab initio crystal prediction methods. Crystalline space groups in which minimizations were performed are denoted by the symbols defined in the legend.

within 3 kcal/mol of the GM, and as a result of lattice minimization, 48% of these (namely 2.2% from the total number) have converged to the same energy minimum (the GM) after minimization. For this crystal, it has also been found that the structure corresponding to the GM has also the highest density among the series of hypothetical crystals. In contradistinction to the RDX case, we have also found several situations where the lattice energies of the hypothetical crystals are almost equal to the GM despite significant differences in the symmetries and crystallographic parameters of these structures. Such a case is the METNAM22 crystal (hexadeutero-*N*,*N*-dimethyl-nitramine, see entry 90 in Table 2S), also illustrated in Figure 2. In this case, the range of lattice energies of the predicted hypothetical crystals is 4.5 kcal/mol, whereas 99% of the hypothetical crystals have lattice energies within 3 kcal/mol of the global minimum (GM). The GM for METNAM22 is identified as the Match to the experimental crystal having the monoclinic $P2_1/c$ symmetry. The local minimum with energy closest to the GM identified by the MOLPAK/WMIN procedure has space group symmetry $P\bar{1}$ and is separated by only 0.02 kcal/mol from the GM (see Table 1). Symmetry-constrained normal-mode analyses confirmed that these energy minima are different.

Beside the situations presented for the RDX and METNAM22 crystals, there were also systems for which two or more MOLPAK structures resembled the experimental structure but differed only slightly in crystallographic parameters rather than in lattice energies. In one such case, NXENAM01 (2,2′-dinitroxydiethylnitramine, entry 97 in Table 2S), a higher-energy MOLPAK structure (by 0.32 kcal/mol) more closely matched the experimental structure than the low-energy structure (see Table 1). Since the crystallographic parameters and energies of the two structures are so close, symmetry-constrained normal-mode analyses were performed to ensure that the extrema located in the optimization procedure were true energy minima. The corresponding eigenvalues for the two crystals were all positive, and the two sets of eigenvalues were not identical, indicating that the two energy minima corresponded to two different crystal structures. It is not known whether the existence of these local minima and their similarities in energies and structures are artifacts of the simple classical pair potentials used in this study. Alternatively, it is possible that inclusion of flexibility of the molecules in the packing calculations could influence the final structure, packing and energy rankings. Although these points invite further research, we do not address these in this study.

Ideally, first principles calculations of the interatomic interactions in a molecular crystal could be used to characterize the local minima on the potential energy surface; however, practical constraints preclude their use at the present time. The current solid state density functional theory implementations, when applied to some energetic molecular crystals, are unreliable, most likely due to inadequate treatment of dispersion interactions.[35−36] Other ab initio theories that could properly treat dispersion, such as MP2,[15−20,36] are too computationally demanding to be used at this time.

Identification of Matches to Experimental Crystals. In most cases, the best match of MOLPAK predictions to experiment is easily determined, and the superposition of the MOLPAK match to experiment is so good that, visually, the molecules are indistinguishable. Such a case is, for example, the BECJEY (2,3-dimethyl-2,3-dinitrobutane) crystal represented in Figure 3a. However, there were a few cases in which the molecular orientations and mass positions within the cell had larger differences from experiment (as seen in Table 3S). Such an example is illustrated in Figure 3b for the case of the DNEDAM crystal.

The MOLPAK/WMIN calculations generated crystals that matched the experimental structure for 148 of the 174 systems studied (85%). Eight of the 148 matches were found only after performing a second set of calculations in which the test molecule is reoriented about each of the Eulerian axes in increments of 5° during the MOLPAK portion of the calculations. 75% (111) of the 148 matches have the lowest lattice energy of all candidate crystals generated in the MOLPAK/WMIN procedure. Table 2S also provides the lattice energies of these crystals identified as matches to experiment and the energy differences (if any) relative to the GM structures.

Another point we have investigated in this study is whether the aforementioned statistics on the capability of the MOLPAK/WMIN procedure to identify crystal structures consistent with experiment are dependent on the chemical classes of CHNO crystals included in this study, i.e., nitramines, nitroaliphatics, nitroaromatics, and nitrate esters. In performing this analysis, we need to point out that several systems have been included in more than one category since many of them have multiple NO_2 groups that are attached to different atom types. For example, the ENPROP (ethyl 3-nitrato-2-nitro-3-(4-nitrophenyl)-propionate) crystal has NO_2 groups attached to oxygen, an aliphatic carbon and an aromatic carbon. Therefore, in the subsequent analyses, ENPROP is categorized as a nitrate ester, a nitroaliphatic and a nitroaromatic system.

Nitramines. This category contains 77 crystals that were subjected to ab initio crystal prediction. Of these, 84% (65) were identified as a match to experiment by the MOLPAK/WMIN procedure. 78% (51) of the crystals identified as matches to experiment correspond to the global energy minimum.

Nitroaliphatic. 85% (56) of the 66 candidates in this category were identified as matches to the experimental systems by the MOLPAK/WMIN procedure; of these, 73% (41) correspond to the global energy minimum.

Nitroaromatic. 27 out of 29 of the systems in this category (93%) were identified as matches to experiment. Of these, 78% (21) correspond to the global energy minimum

Nitrate Esters. Of the 33 crystals in this category, 85% (28) were identified as matches to the experimental crystals; 79% of these (22 out of 28) correspond to the global energy minimum.

Separate analyses were not performed for systems that could be categorized as furoxans or systems containing azido or nitroso

TABLE 1: Comparison of the Predicted Crystallographic Parameters for Crystals with Similar Lattice Energies or Structural Parameters[e]

crystal	space group	density[a] (g/cm^3)	a (Å)[a]	b (Å)[a]	c (Å)[a]	α (deg.)[b]	β (deg.)[b]	γ (deg.)[b]	$\Delta\theta$ (deg.)	Δx (Å)	E (kcal/mol)
CTMTNA	*Pbca*[c]	1.806	10.709	11.574	13.182	90.00	90.00	90.00			
	Pbca[d]	1.800 (−0.3)	10.6144 (−0.9)	11.6359 (0.5)	13.2700 (0.7)	90.00 (0.00)	90.00 (0.00)	90.00 (0.00)	1.4	0.06	−31.92
	Pbca[d]	1.774 (−1.8)	10.6582 (−0.5)	11.6493 (0.7)	13.3949 (1.6)	90.00 (0.00)	90.00 (0.00)	90.00 (0.00)	9.6	0.64	−31.05
METNAM22	*P*21/*c*[c]	1.564	6.180	6.540	10.090	91.21	90.00	90.00			
	*P*21/*n*[d]	1.404	6.2301	6.6211	10.3354	92.212	90.00	90.00			−17.03
	$P\bar{1}$[d]	1.403	6.0398	6.2321	6.2497	88.349	65.130	87.498			−17.01
NXENAM01	*P*21/*c*[c]	1.660	9.060	9.150	12.330	90.00	109.94	90.00			
	*P*21/*c*[d]	1.676 (0.9)	9.0486 (−0.1)	9.0942 (−0.6)	12.3427 (0.1)	90.00 (0.00)	110.41 (0.47)	90.00 (0.00)	1.3	0.03	−32.20
	*P*21/*c*[d]	1.684 (1.5)	8.8580 (−2.2)	9.0646 (−0.9)	12.3405 (0.1)	90.00 (0.00)	107.10 (−2.84)	90.00 (0.00)	4.0	0.06	−32.54

[a] Percent difference from experiment given in parentheses. [b] Difference from experiment (in degrees) given in parentheses. [c] Experimental information. [d] Hypothetical crystals generated from MOLPAK/WMIN calculations. [e] The lattice parameters are given for the reduced unit cells.

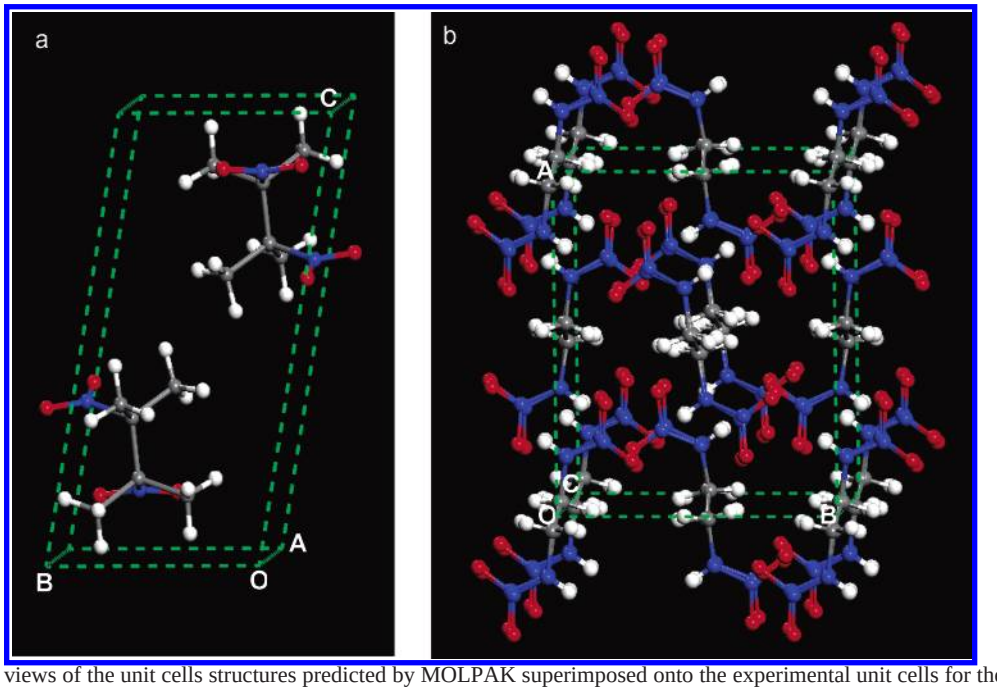

Figure 3. Pictorial views of the unit cells structures predicted by MOLPAK superimposed onto the experimental unit cells for the (a) BECJEY and (b) DNEDAM crystals. The cell vectors correspond to the experimental values.

groups, due to the small numbers of these types of systems studied. The above results indicate that, in terms of identification of the experimental structure, the method and SRT model behave fairly consistently across all categories investigated with a success rate of about 85% for the nitramine, nitroaliphatic, and nitrate ester categories and an even slightly higher success rate for the nitroaromatic class of 93%. This consistency is also observed with regard to the percentages of the identified matched systems corresponding to the global minimum. In this case, the success rate ranges from 73% to 79%.

For the 37 matches that did not have the lowest lattice energy among the possible candidates, all but six had lattice energies within 1 kcal/mol of the global energy minimum. The largest difference in energy between the match to experiment and the structure with lowest lattice energy is for PERYTN01 (2.86 kcal/mol). This particular result could be indicative of deficiencies in the SRT force field for this system. However, for this system, no R factor was recorded; so it is also possible that the structure is not well characterized at the experimental conditions.

An additional analysis was performed to determine whether failures of the search method clustered into particular space groups. For the most part, no clustering of failures occurred in any particular space group. For each individual space group analyzed by MOLPAK, we determined that 80 to 100% of the systems with that space group produced matches to the experimental structures. An exception from these statistics was seen for the case of *Pca*21 crystal symmetry which had a success rate of 50%. However, in this case, there were only four systems with this space group symmetry.

5.1. Structural Predictions. Results of the MOLPAK/WMIN predictions of structural parameters for crystals identified as best matches to the experiment are given in Table 3S and illustrated in Figures 4−6. Figure 4a shows the percent deviation in density of the MOLPAK predictions compared to experimental values for the entire set of molecules. Overall, the MOLPAK densities are overestimated on average by 2.8% and have a rms deviation of 3.9%. Also, in the great majority of cases, namely 131 out of 148, the predicted crystal densities were found to be larger than the corresponding experimental values. This is not surprising, since the MOLPAK/WMIN predictions reflect simple energy minimizations that do not include thermal effects, and the majority of the crystal structural parameters were determined at room temperature (see Table 1S). Earlier NPT-MD simulations for a few of the systems studied herein predicted expansion of the lattice (i.e., a decrease in density) when thermal effects are included.[1,3−4,6] Therefore, the MOLPAK/WMIN results should be considered as upper limits to predictions of density, assuming that no unusual thermal expansion behavior exists.

The percent differences in density between predictions and experiment for the four categories of CHNO crystals analyzed in this study are illustrated in Figure 4b−e. The nitroaromatic category has the smallest rms deviation of predictions of density

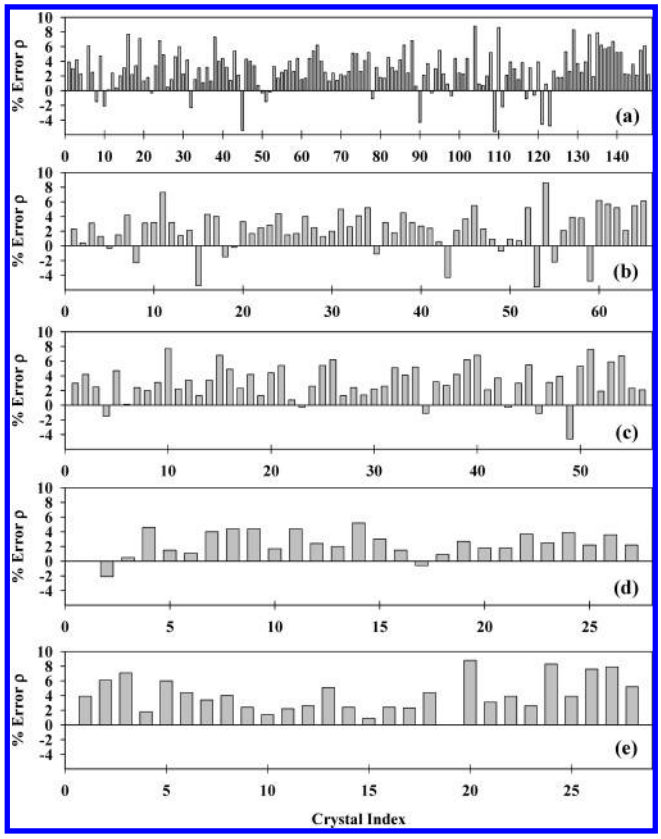

Figure 4. Calculated percentage errors between the predicted and experimental values of the densities for (a) entire set of crystals; (b) nitramine crystals; (c) nitroaliphatic crystals; (d) nitroaromatic crystals; and (e) nitrate ester crystals. The crystal indices for each frame correspond to those given in Table 3S.

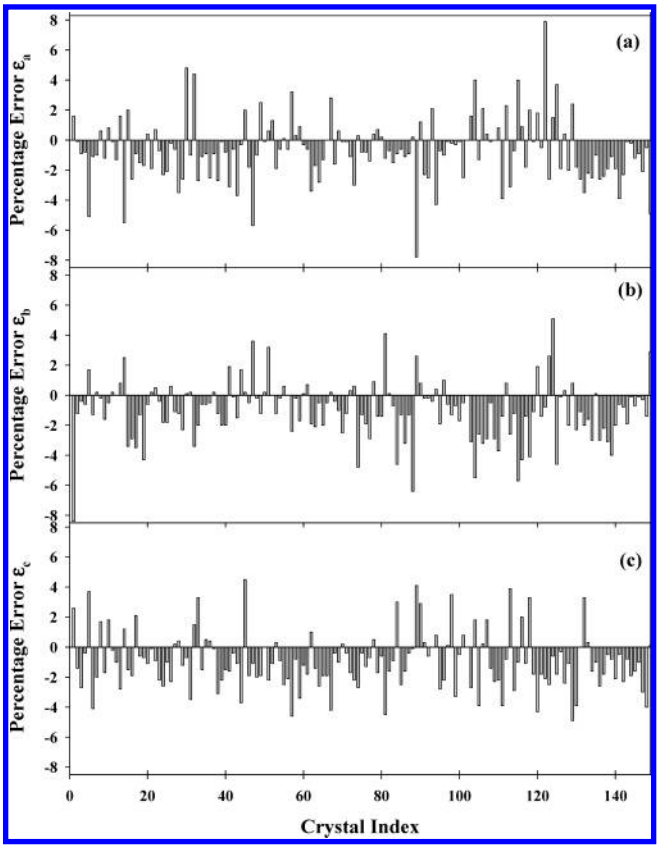

Figure 5. Calculated percentage errors between the predicted and experimental values of the lattice dimensions *a* in (a), *b* in (b), and *c* in (c) for all crystals given in Table 3S.

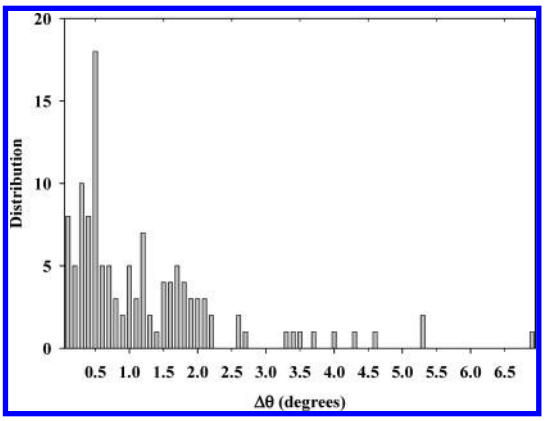

Figure 6. Distribution of absolute differences in cell angles (in degrees) between predictions and measured values for all non-90° angles.

from experiment (2.9%), and the nitrate ester class had the largest (4.7%). The rms deviations of the predictions of density from experimental values for the nitramine and nitroaliphatic classes are 3.6 and 4.0%, respectively. Average percent deviations of density between the MOLPAK/WMIN predictions and experiment are 2.3, 3.1, 2.3, and 4.1% for the nitramine, nitroaliphatic, nitroaromatic, and nitrate ester classes, respectively.

The percent differences in lattice dimensions between the predictions and experiment are shown in Figure 5. The results indicate that for the majority of the crystals the predicted lattice dimensions are smaller than those of the experiment. The average percent differences for the cell edge lengths *a*, *b*, and *c* are all −1%, whereas the corresponding rms deviations of percent differences are 2.2, 2.2, and 2.1%, respectively.

Since the symmetry of the crystals is constrained during the MOLPAK/WMIN calculations, orthorhombic and monoclinic systems have some or all cell angles fixed at 90° and were not allowed to vary during the packing/minimization procedure. Thus, these angles were not included in the distribution of absolute differences in predictions of cell angles from experimental values shown in Figure 6. The total number of nonfixed cell angles used in the distribution is 122. Among these, about 88% of cell angles deviate from the experiment by no more than 2°. The largest differences in predicted cell angles from experimental values are −5.15° for DACYEL (3,5-diamino-2,4,6-trinitrobenzoic acid), 5.17° for DETDOV (2-nitro-6,7,8,9-tetrahydronaphtho(2,1-b)furan), and 6.82° for KEDWAR (3-isopropyl-6-methyl-t-5-nitrato-1,r-3,c-4,c-6-tetranitrocyclo-hexene).

Regarding molecular orientation, the rms rigid-body rotational displacement and translational displacement after minimization for the entire set of crystals are 1.9° and 0.07 Å, respectively. The rms translational displacement for each of the nitramine, nitroaliphatic, nitroaromatic, and nitrate ester classes is 0.07 Å. The corresponding rms rigid-body rotational displacements for the same four categories are 2.1, 1.8, 2.0, and 1.6°, respectively.

The calculations have demonstrated that for at least two systems in which strong intermolecular hydrogen bonding is present, namely, TATNBZ (1,3,5-triamino-2,4,6-trinitrobenzene, entry 119 in Table 2S) and SEDTUQ01 (1,1-diamino-2,2-dinitroethylene, entry 117 in Table 2S), the predictions of crystallographic parameters by SRT potential are less accurate than those obtained for other classes of energetic materials, such as the nitramines. In an earlier MP and NPT-MD study on the SEDTUQ01 (FOX-7) crystal,[37] Sorescu et al. showed that the SRT model did not reproduce accurately the measured crystal parameters for this system. Sorescu et al. refitted the attractive-repulsive N−N and O−O potential terms in order to get better

agreement with experiment; molecular simulations of the system produced a suitable result. Another way to overcome the inadequacies in the SRT model in describing hydrogen-bonded systems might be to treat the electrostatic interactions as an expansion of atom-centered multipoles, rather than that of atom-centered point charges. It has been shown that for hydrogen-bonded structures, $\pi-\pi$ interactions, or polar crystals incorporation of distributed higher multipoles for description of the electrostatic interactions will result in more accurate predictions of crystal structures.[38−40]

5.2. Problem Cases. We have indicated in previous sections that the MOLPAK/WMIN procedure in conjunction with the SRT potential was able to match the experimental structure for 148 out of 174 systems studied. In this section, we focus our efforts on possible sources of failure for the remaining 26 crystals. Particularly, in an attempt to determine whether the failure to identify the 26 of the 174 crystals was due to inadequacies in the SRT intermolecular interaction potential or in the search method, we performed geometry optimizations of the 26 crystals using the experimental crystals as initial structures in the MP calculations. Each calculation resulted in convergence to a local energy minimum and the corresponding crystal structure was superimposed on the experimental structure in the manner described in section 4.3. Although there are notable disagreements in the predicted crystallographic parameters and molecular orientations with the experiment, the predicted crystals resemble the experimental systems. Crystallographic parameters and rms rigid-body rotational and translational displacements are given in Table 4S. In all cases, the predicted crystal densities were found to be smaller than the corresponding experimental values and on average underestimated the experimental values by 2.9%. This is in contrast to the results for systems identified through the MOLPAK procedure; in those cases, 89% of the systems had densities that were larger than the experiment. The rms deviation of the density for these problem case crystals is 3.6% [Figure 7a]. The percent differences in lattice dimensions between the predictions and experiment are also given in Figure 7b−d. Average percent differences for the cell edge lengths *a*, *b*, and *c* are −2.8, −2.5, and −2.8%, respectively, whereas the corresponding rms deviations of percent differences are 4.3, 3.4, and 5.0%, respectively. The rms rigid-body rotational and translational displacements after minimization for this set of crystals are 3.6° and 0.13 Å. Overall, these results indicate that the SRT potential did a poorer job of representing these systems. Two systems were particularly poorly described by the SRT potential: NOGUNA01 (*N*-methyl-*N*-nitroso-N′-nitroguanidine) and JIHVEB [(*E*)-acetonitrolic acid]. For example, we have seen deviation of the cell edge lengths as high as 19.7% for NOGUNA01 and 10.76% for JIHVEB. Also, GEJXAU (1,7-dimethyl-1,3,5,7-tetranitrotrimethylenetetramine), one of the systems in which hydrogen atoms were supplemented due to lack of experimental information in the CSD, was not identified in the MOLPAK search. Subsequent optimization to a local energy minimum when starting with the assumed experimental molecule structure (with the supplemented hydrogen atoms) indicates that this failure is not due solely to improper placement of the hydrogen atoms.[30]

Beside deficiencies of the potential used in simulation of these crystals we note that another reason some of the searches might have been unsuccessful is due to the existence of several local minima on the potential energy surface landscape. As a result, optimization of one of the candidate crystals generated during the search procedure might be prevented from reaching the GM or the local minimum corresponding to the experimental crystal due to convergence to one of the other local minima. In such an instance, the identification of a local minimum corresponding to the experimental structure is precluded. Beyer, Lewis, and Price have suggested that the search procedure is flawed for those cases in which a local minimum with structural parameters close to experiment exists but which is not found during the search procedure.[26−27] Our results have clearly demonstrated that for the problem cases there are several local minima with structural parameters significantly different from those of the experimental structure. Since the direct minimization of the experimental structure for each of the problem cases resulted in convergence to a local minimum with structural parameters resembling the experiment, the failure to identify these minima in the MOLPAK/WMIN procedure suggests that the search procedure is not fully adequate for these cases.

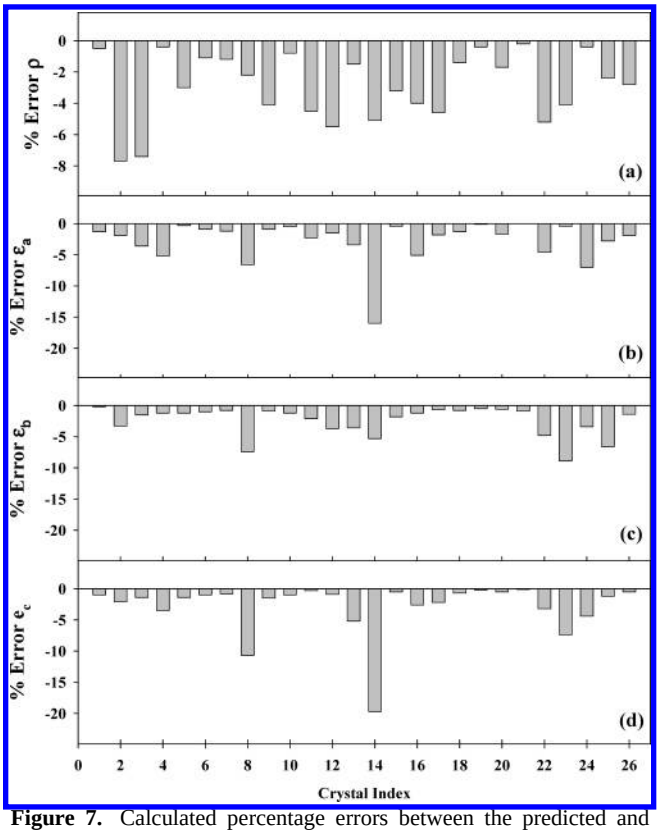

Figure 7. Calculated percentage errors between the predicted and experimental values of the densities (a) and lattice dimensions *a* in (b), *b* in (c), and *c* in (c) for the set of crystals that were not identified by the MOLPAK search procedure. The crystal indices for each frame correspond to those given in Table 4S.

A few (four) of the systems identified as matches to the experiment had deviations from experimental values of individual cell lengths greater than 6%, which probably cannot be attributed to thermal expansion effects. These systems are ACANOH [2-(isonicotinoylamino)ethyl nitrate], MENFXN (3-methyl-4-nitrofuroxan), MENOGU (*N*-methyl-N′-nitroguanidine), and TEVHEH (2,4-dinitroimidazole). We have not been able to identify any particular correlation between the chemical groups or the type of bonding of these crystals to motivate the observed errors in the cell parameters.

6. Summary and Conclusions

A total of 174 CHNO crystals for which experimental crystallographic information is available were subjected to ab initio crystal prediction using the MOLPAK/WMIN suite of software[8,9] and the Sorescu−Rice−Thompson (SRT) interaction potential for CHNO crystals.[1] The systems under study consist

of nitramine, nitroaliphatic, nitroaromatic, and nitrate ester molecules and included a variety of acyclic, monocyclic, and polycyclic/caged species. The calculations produced 148 crystals whose crystallographic parameters and molecular configurations matched those of the experimental counterpart. Of these, 75% corresponded to the global energy minimum on the potential energy surface. Predicted structural parameters of the matches were in good agreement with experimental values; predicted densities were, on average, higher than those of the experiment by less than 3%, and cell edge lengths deviated from those of the experiment on average by no more than −1%. Rigid body rotational and translational displacements had rms deviations from those of the experiment of 1.9° and 0.07 Å, respectively. For the 26 systems that were not identified by the MOLPAK search procedure, energy minimizations were performed using experimental geometries as the initial structures. A local energy minimum was found for each case, and the corresponding crystal structures resembled the experimental systems. However, differences between predicted and experimental crystallographic parameters were larger on average than for the systems identified by the MOLPAK/WMIN procedure.

For each of the chemical CHNO classes studied in this work, namely nitramines, nitroaliphatic, nitroaromatic, and nitrate esters, we found similar statistics regarding identification of crystal and structural parameters. A slightly higher percent deviation of density from experiment was found for the nitrate ester class. The uniformity of the statistics for the four categories of CHNO crystals that were identified in the MOLPAK/WMIN procedure indicates that the SRT interaction potential is transferable among these classes of compounds. Consequently, this assessment provides a level of confidence in the SRT model when applied to these classes of CHNO compounds.

The overall good performance of the MOLPAK/WMIN procedure and SRT potential in identifying the experimental systems and producing relatively good agreement with structural parameters for 85% of the systems studied demonstrates that both the model and method are reasonable to use in ab initio crystal predictions of similar CHNO systems when the molecular configuration is known.

Acknowledgment. The authors thank Dr. Antonio Santoro, National Institute of Standards and Technology, for valuable discussions and Dr. Herman L. Ammon, University of Maryland, for providing the MOLPAK/WMIN suite of codes and helpful advice. This work was supported in part by the DOD High Performance Computing Software Support Initiative (CHSSI) for Computational Chemistry and Material Science (MBD-4).

Supporting Information Available: Ab initio MP results obtained for the entire set of 174 molecular crystals (Tables 1S−4S). This material is available free of charge via the Internet at http://pubs.acs.org.

References and Notes

(1) Sorescu, D. C.; Rice, B. M.; Thompson, D. L. *J. Phys. Chem. B* **1997**, *101*, 798.

(2) Williams, D. E. PCK91, *A Crystal Molecular Packing Analysis Program*; Department of Chemistry, University of Louisville: Louisville, KY.

(3) Sorescu, D. C.; Rice, B. M.; Thompson, D. L. *J. Phys. Chem. B* **1998**, *102*, 948.

(4) Sorescu, D. C.; Rice, B. M.; Thompson, D. L. *J. Phys. Chem. B* **1998**, *102*, 6692.

(5) Sorescu, D. C.; Rice, B. M.; Thompson, D. L. *J. Phys. Chem. A* **1998**, *102*, 8386.

(6) Sorescu, D. C.; Rice, B. M.; Thompson, D. L. *J. Phys. Chem. A* **1999**, *103*, 989.

(7) Sorescu, D. C.; Rice, B. M.; Thompson, D. L. *J. Phys. Chem. B* **1999**, *103*, 6783.

(8) Holden, J. R.; Du, Z.; Ammon, H. L. *J. Comput. Chem.* **1993**, *14*, 422.

(9) Busing, W. R. *WMIN, A Computer Program to Model Molecules and Crystals in Terms of Potential Energy Functions;* Report ORNL-5747, Oak Ridge National Laboratory: Oak Ridge, TN, 1981.

(10) Allen, F. H. *Acta Crystallogr.* **2002**, *B58*, 380.

(11) Frisch, M. J.; Trucks, G. W.; Schlegel, H. B.; Scuseria, G. E.; Robb, M. A.; Cheeseman, J. R.; Montgomery, J. A., Jr.; Vreven, T.; Kudin, K. N.; Burant, J. C.; Millam, J. M.; Iyengar, S. S.; Tomasi, J.; Barone, V.; Mennucci, B.; Cossi, M.; Scalmani, G.; Rega, N.; Petersson, G. A.; Nakatsuji, H.; Hada, M.; Ehara, M.; Toyota, K.; Fukuda, R.; Hasegawa, J.; Ishida, M.; Nakajima, T.; Honda, Y.; Kitao, O.; Nakai, H.; Klene, M.; Li, X.; Knox, J. E.; Hratchian, H. P.; Cross, J. B.; Adamo, C.; Jaramillo, J.; Gomperts, R.; Stratmann, R. E.; Yazyev, O.; Austin, A. J.; Cammi, R.; Pomelli, C.; Ochterski, J. W.; Ayala, P. Y.; Morokuma, K.; Voth, G. A.; Salvador, P.; Dannenberg, J. J.; Zakrzewski, V. G.; Dapprich, S.; Daniels, A. D.; Strain, M. C.; Farkas, O.; Malick, D. K.; Rabuck, A. D.; Raghavachari, K.; Foresman, J. B.; Ortiz, J. V.; Cui, Q.; Baboul, A. G.; Clifford, S.; Cioslowski, J.; Stefanov, B. B.; Liu, G.; Liashenko, A.; Piskorz, P.; Komaromi, I.; Martin, R. L.; Fox, D. J.; Keith, T.; Al-Laham, M. A.; Peng, C. Y.; Nanayakkara, A.; Challacombe, M.; Gill, P. M. W.; Johnson, B.; Chen, W.; Wong, M. W.; Gonzalez, C.; Pople, J. A. *Gaussian 03*, revision A.1; Gaussian, Inc.: Pittsburgh, PA, 2003.

(12) Becke, A. D. *J. Chem. Phys.* **1993**, *98*, 5648.

(13) Lee, C.; Yang, W.; Parr, R. G. *Phys. Rev.* **1988**, *B41*, 785.

(14) Hariharan, P. C.; Pople, J. A. *Theor. Chim. Acta* **1973**, *28*, 213.

(15) Möller, C.; Plesset, M. S. *Phys. Rev.* **1934**, *46*, 618.

(16) Head-Gordon, M.; Pople, J. A.; Frisch, M. J. *Chem. Phys. Lett.* **1988**, *153*, 503.

(17) Frisch, M. J.; Head-Gordon, M.; Pople, J. A. *Chem. Phys. Lett.* **1990**, *166*, 275.

(18) Frisch, M. J.; Head-Gordon, M.; Pople, J. A. *Chem. Phys. Lett.* **1990**, *166*, 281.

(19) Head-Gordon, M.; Head-Gordon, T. *Chem. Phys. Lett.* **1994**, *220*, 122.

(20) Sæbø, S.; Almlöf, J. *Chem. Phys. Lett.* **1989**, *154*, 83.

(21) Gavezzotti, A. *Acc. Chem. Res.* **1994**, *27*, 309.

(22) Gdanitz, R. J. In *Theoretical Aspects and Computer Modeling*; Gavezzotti, A, Ed.; John Wiley & Sons Ltd.: New York, 1997; p 185.

(23) Verwer, P.; Leusen, F. J. J. In *Reviews in Computational Chemistry*; Lipkowitz, K. B., Boyd, D. B., Ed.; Wiley-VCH: New York, 1998; p 327.

(24) Gdanitz, R. J. *Curr. Opin. Solid State Mater. Sci.* **1998**, *3*, 414.

(25) Gavezzotti, A. *Synlett* **2002**, 201.

(26) Beyer, T.; Lewis, T.; Price, S. L. *Cryst. Eng. Comm* **2001**, *44*, 1.

(27) Lommerse, J. P. M.; Motherwell, W. D. S.; Ammon, H. L.; Dunitz, J. D.; Gavezzotti, A.; Hofmann, D. W. M.; Leusen, F. J. J.; Mooij, W. T. M.; Price, S. L.; Schweizer, B.; Schmidt, M. U.; van Eijck, B. P.; Verwer, P.; Williams, D. E. *Acta Crystallogr.* **2000**, *B56*, 697.

(28) Motherwell, W. D. S.; Ammon, H. L.; Dunitz, J. D.; Dzyabchenko, A.; Erk, P.; Gavezzotti, A.; Hofmann, D. W. M.; Leusen, F. J. J.; Lommerse, J. P. M.; Mooij, W. T. M.; Price, S. L.; Scheraga, H.; Schweizer, B.; Schmidt, M. U.; van Eijck, B. P.; Verwer, P.; Williams, D. E. *Acta Crystallogr.* **2002**, *B58*, 647.

(29) Mooij, W. T. M.; van Eijck, B. P.; Price, S. L.; Verwer, P.; Kroon, J. *J. Comput. Chem.* **1998** *19*, 459.

(30) Hofmann, D. W. M.; Lengauer, T. *J. Mol. Model.* **1998**, *4*, 132.

(31) Cromer, D. L.; Ammon, H. L.; Holden, J. R. *A Procedure for Estimating the Crystal Densities of Organic Explosives*; Report LA-11142-MS, Los Alamos National Laboratory: Los Alamos, NM, 1987

(32) Santoro, A.; Mighell, A. D. *Acta Crystallogr.* **1970**, *A 26*, 124

(33) Kearsley, S. K. *Acta Crystallogr.* **1989**, *A45*, 208.

(34) Gavezzotti, A.; Filippini, G. *J. Am. Chem. Soc.* **1995**, *117*, 1229.

(35) Byrd, E. F. C.; Scuseria, G. E.; Chabalowski, C. F. *J. Phys. Chem. B* **2004**, *108*, 13100.

(36) Shaw, R. *Tools for Condensed Phase Computational Chemistry*; ARO Report, http://www.aro.army.mil/chemb/people/shaw.htm, 2003.

(37) Sorescu, D. C.; Boatz, J. A.; Thompson, D. L. *J. Phys. Chem. A* **2001**, *105*, 5010.

(38) Day, G. M.; Price, S. L.; Leslie, M. *Cryst. Growth Des.* **2001**, *1*, 13.

(39) Price, S. L.; Stone, A. J. *Mol. Phys.* **1984**, *51*, 569.

(40) Willock, D. J.; Price, S. L.; Leslie, M.; Catlow, C. R. A. *J. Comput. Chem.* **1995**, *16*, 628.